Statistical Behavior of ALACE Floats at the Surface of the Southern Ocean

SARAH T. GILLE

Scripps Institution of Oceanography and Department of Mechanical and Aerospace Engineering, University of California, San Diego, La Jolla, California

LEONEL ROMERO

Scripps Institution of Oceanography, University of California, San Diego, La Jolla, California

(Manuscript received 17 April 2002, in final form 18 December 2002)

ABSTRACT

Autonomous Lagrangian Circulation Explorer (ALACE) floats were designed to measure subsurface velocities throughout the global ocean. In order to transmit their data to satellite, they spend 24 h at the ocean surface during each 10–25-day cycle. During this time the floats behave as undrogued drifters. In the Southern Ocean, floats tend to advect downwind and, in accordance with Ekman theory, slightly to the left of the wind during their time at the surface. Mean displacements are likely to carry floats northward and, correspondingly, with each cycle, the Southern Ocean floats will move into warmer water with higher dynamic height. Because of large variability, the northward trend may not be discernible for any single float: in 2 years' worth of 10-day cycles, a typical float will be displaced 100 ± 270 km northward relative to a float that never surfaces. Float surface velocities and wind speed are statistically correlated at the 95% confidence level. Compared with drogued drifters, floats tend to move more rapidly, are advected more strongly downwind, and are more sensitive to changes in wind speed. Regression coefficients estimated from the differences between float and drogued drifter velocities suggest that floats may be used to estimate the mean upper ocean currents in regions where drogued drifter data are not available.

1. Introduction

Autonomous Lagrangian Circulation Explorer (ALACE) floats were developed in the late 1980s and have been deployed globally since the early 1990s to study middepth ocean circulation (Davis 1992, 1998). The success of the ALACE floats has led to a number of successor float designs, now being deployed through the Argo float program. The floats are equipped with an inflatable bladder and a pump so that they can adjust their buoyancy to travel between the surface and a fixed depth below the surface. ALACE floats spend most of their time at middepth, typically about 900 m, but are programmed to rise to the surface every 10–25 days in order to transmit to satellite their position, mean temperature, and, in some cases, vertical temperature and salinity profiles. Using current technology, floats spend about 24 h at the surface in order to contact an Argos system satellite and relay all of their information. This study focuses on the behavior of ALACE floats at the ocean surface.

Corresponding author address: Dr. Sarah T. Gille, Scripps Institution of Oceanography, Department of Mechanical and Aerospace Engineering, University of California, San Diego, La Jolla, CA 92093-0230.
E-mail: sgille@uscd.edu

In order to ensure that their antennas are above the water so that they can reliably contact the Argos satellites, ALACEs are designed to have substantial buoyancy at the ocean surface (Davis 1992). Because the floats have no underwater drogue and ride far above the waterline, they tend to behave like undrogued surface drifters. Thus they are expected to be accelerated by the winds and waves and therefore are unlikely to follow the motions of water parcels in the upper ocean (Pazan 1996).

Since ALACE floats may be displaced substantially by the wind at the surface and by surface intensified currents, they do not necessarily rejoin the same middepth streamline or water mass on consecutive dives. Therefore, most studies have treated successive velocity estimates from the same float as statistically independent and unrelated quantities (Davis et al. 1996; Davis 1998; Gille 2003). However, the actual behavior of the floats at the surface has not been quantified, and some indications suggest that the trajectories obtained from each of the ALACE floats may resemble trajectories from nonsurfacing floats (LaCasce 2000).

Rather than analyzing data from the entire globe, in this study we specifically concentrate on the Southern Ocean, although we expect that these results should extend to the global ocean. Section 2 discusses the data

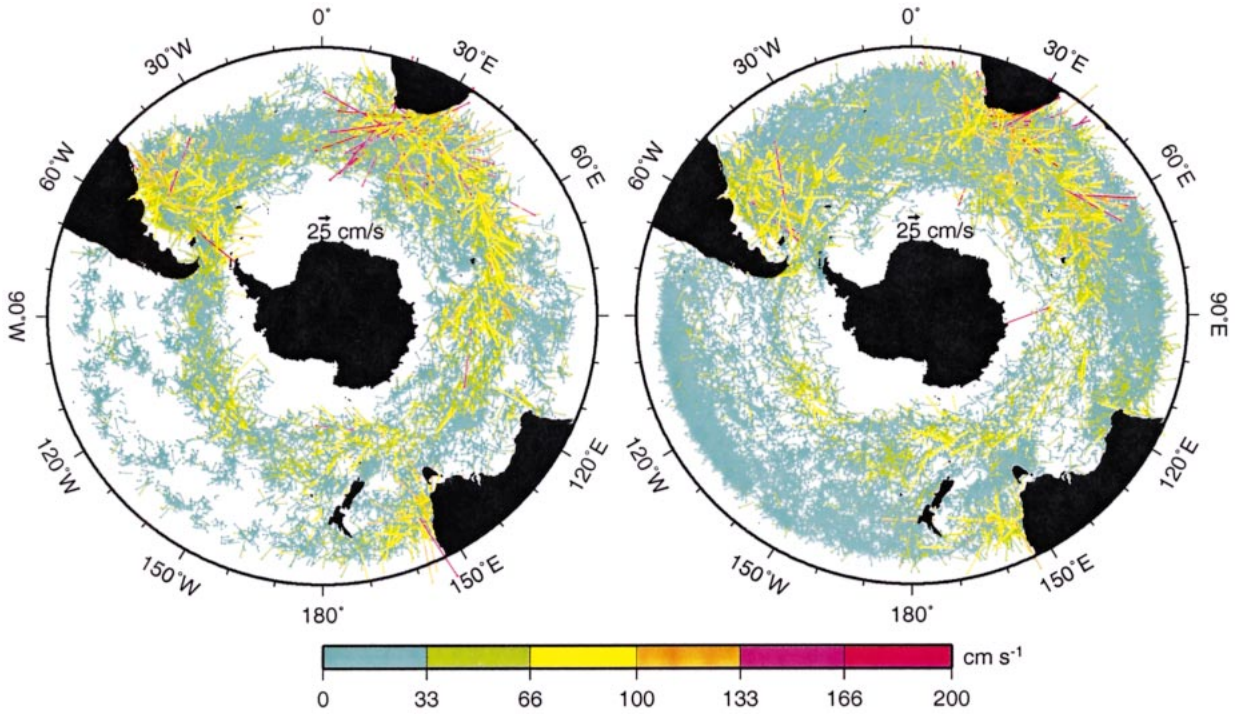

FIG. 1. Geographical distribution of float and drifter data in the Southern Ocean: (left) ALACE float surface velocities between 1990 and 2000 and (right) drogued surface drifter velocities between 1989 and 2000.

used in this study. In section 3, we quantify the displacement of ALACE floats by surface currents as well as wind and wave motions. Section 4 examines the possibility of removing the wind slip from ALACE surface velocities, in much the way that wind slip is removed from undrogued surface drifters, in order to study upper-ocean circulation. Results are summarized in section 5.

2. Data

a. ALACE floats

For this study, we analyzed a total of 15 027 velocity observations from 302 ALACE floats operating in the Southern Ocean between 1990 and 2000. Surface velocities inferred from these records are shown in Fig. 1 (left). These represent mean velocities averaged over the 24-h period that the floats spend at the surface. Davis (1998) estimated the uncertainty in surfacing and diving positions to be 1–3 km. Observations are densest in the South Atlantic, where substantial numbers of floats were deployed, and in the Antarctic Circumpolar Current (ACC), where strong currents advect floats rapidly to provide extensive spatial coverage. The mean surface speed of the floats was 25.9 ± 0.8 cm s^{-1}, and their mean direction at the surface was 6.7° ± 1.2° to the north of due east. (Here, and throughout this paper, error bars assigned to means are standard errors, computed as $2\sigma/\sqrt{N}$, where σ is the standard deviation and N the number of independent samples.)

In order to evaluate how surface motions differ from subsurface motions at the same time and place, we examined the angular difference between surface motions and the subsurface float velocities observed immediately before and after surfacing. Since eastward winds are likely to drive northward Ekman transports everywhere, we restricted this analysis to times when subsurface velocities indicated eastward advection (with motions between ±90° of due east). In these cases, surface velocities are rotated toward the north by an average of 3° ± 1° relative to subsurface velocities.

b. Mean temperature and dynamic height

We compared ALACE float data with surface and subsurface temperature and dynamic height. These data were derived from the atlas compiled by Gouretski and Jancke (1998), gridded at 1° resolution, and dynamic height was computed relative to 3000-m depth. Temperature and dynamic height contours both run predominantly from west to east. For example, at the locations where floats rise to the surface, surface temperature contours have a mean orientation of −0.5° ± 0.3° just barely south of due east, and surface dynamic height contours are oriented 4.3° ± 0.4° slightly to the north of due east.

c. Wind fields

In order to examine float response to wind forcing, we used 10-m wind fields derived from the National

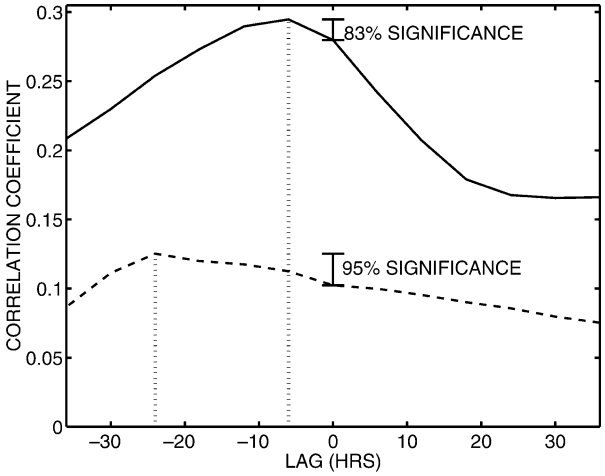

FIG. 2. (solid line) Correlation coefficient of wind speed and along-wind component of float velocity as a function of the time separation between wind and float observations. (dashed line) Same but for wind speed vs the crosswind component of float velocity.

Centers for Environmental Prediction (NCEP) reanalysis (Kalnay et al. 1996). NCEP winds are reported at 6-h intervals, with a spatial resolution of about 1.9°. We used the following procedure to interpolate NCEP winds onto float locations. First, for each 24-h interval that a float spent at the surface, we identified a starting point in time and space, an ending point, and three equally spaced intermediate points. We then linearly interpolated the 6-h winds onto these five points. For each surface displacement, mean winds were determined by averaging the five interpolated winds. Average winds are eastward, with a mean speed of 8.19 ± 0.03 m s^{-1} and a mean orientation of $-7.5° \pm 0.6°$ slightly to the southeast.

Since winds vary slowly in space but rapidly in time, the correlation between float and wind velocities was significantly affected by the temporal averaging technique. Float velocities are more strongly correlated with mean winds computed using interpolated 6-h winds than they are with winds determined from 24-h average wind fields.

In order to verify that winds and floats were well matched, we examined the correlation between wind and float velocities by projecting the float velocities into along-wind and crosswind components. Here the component of wind that is 90° to the left of the wind is denoted as positive crosswind velocity. Figure 2 shows lagged covariances between wind and float velocity components. At zero time lag, the interpolated winds are related to simultaneous along-wind and crosswind float velocities with correlation coefficients of 0.28 and 0.10, respectively. Both correlations are statistically significant at the 99% level (meaning that in no more than 1% of randomly generated datasets would an equivalent level of correlation be observed). The correlation coefficient between winds and along-wind float velocity components increased to 0.30 when winds were 6 h earlier than float velocities, a difference that is significant at the 83% level. For the crosswind float motion, when winds preceded float velocities by 24 h, the correlation coefficient increased to 0.13, a difference that is significant at the 95% level. This suggests that the component of the float motion in the direction of the wind lags the wind by 6 h, while the component of float motion that is perpendicular to the wind responds with a 24-h delay. A 6–12-h delay for the downwind velocity was previously detected in surface drifter data by McNally and White (1985). The fact that crosswind velocities lag the wind can be explained partially by the wind's tendency to rotate anticyclonically: downwind and crosswind components of the wind are most strongly correlated when they differ by 18 h. Other factors contributing to the time lag may include time varying Ekman transport, which responds to a changing wind field by gradually spinning up flow that is perpendicular to the wind (Gill 1982), and frictional effects that dissipate energy input by the wind. For simplicity, this analysis makes use only of the zero-lag wind observations.

d. Surface drifters

Surface drifters supplied with 15-m-deep drogues were used to provide a benchmark in order to evaluate float behavior at the surface. This study employed 12 years of daily drifter observations from the Southern Ocean collected between 1989 and 2000, as depicted in Fig. 1 (right). Drifter coverage is not as extensive as ALACE coverage within the ACC but is more extensive in the region north of the ACC. Drifter data were archived at daily intervals, 6-h NCEP winds were interpolated onto the drifter locations, and drifter data were corrected for wind slip. Details of the drifter data are summarized by Niiler et al. (1995) and by Pazan and Niiler (2001). The drifter velocity observations were calculated to decorrelate in 2–4 days, and the a priori error was estimated to be 0.02 m s^{-1}.

3. Float displacement at the surface

ALACE floats do not lend themselves to the same types of analyses that have been used for traditional subsurface floats (e.g., O'Dwyer et al. 2000; LaCasce 2000), because they spend 24 h at the ocean surface during each 10–25-day cycle. In this section we evalute the distance and direction that ALACE floats travel at the ocean surface.

We analyzed surface float displacements relative to reference fields defined by geographic coordinates, time-mean dynamic height, and time-mean temperature contours. In order to fully consider the changes in float properties as a result of surface displacements, dynamic height, and temperature were examined both at the surface and at 900 m. The subsurface depth of 900 m was chosen to be representative for this study because most

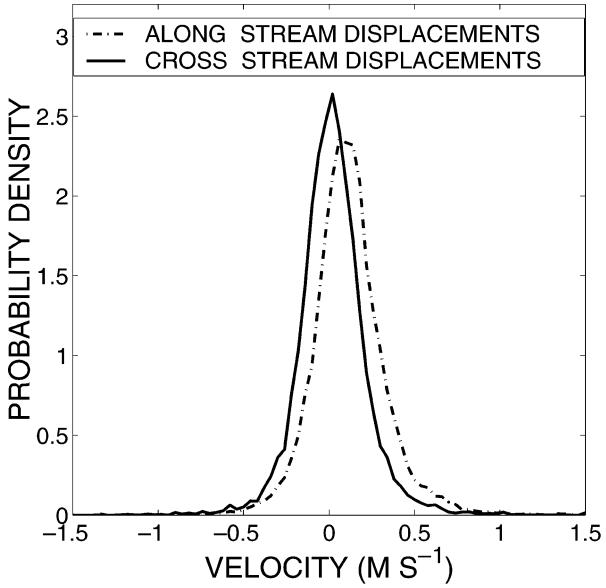

FIG. 3. Probability density functions of ALACE float velocities at the ocean surface. The along-stream velocity component (dashed line) is centered at 0.11 ± 0.04 m s^{-1} and ranges from −1.5 to 1.9 m s^{-1}. The cross-stream velocity component (solid line) has a mean of 0.018 ± 0.004 m s^{-1} and ranges between −1.4 and 1.8 m s^{-1}. Surface displacements are calculated relative to dynamic topography at 900-m depth (referenced to 3000-m depth) from the Gouretski and Jancke (1998) atlas.

of the ALACE floats were ballasted to depths between 700 and 1100 m. Surface float displacements can be represented by two-component vectors oriented relative to the reference fields. The ''along-stream'' component of float displacement is zonal for a reference field defined by geographic coordinates and on average nearly zonal for reference fields defined by dynamic height or temperature. Southern Ocean currents tend to be surface intensified but unidirectional throughout the water column, so mean surface streamlines do not differ substantially from mean subsurface streamlines. The ''cross-stream'' component of float displacement moves floats perpendicular to the reference field.

Figure 3 shows empirical probability density functions (PDFs) of the displacement velocities of ALACE floats at the ocean surface relative to geostrophic streamlines. These PDFs do not differ visibly from PDFs of the displacement velocities relative to temperature contours or geographic coordinates (not shown). Zonal and along-stream velocities (dashed line) show a positive mean, indicating that the surface displacements are eastward, in the same direction as the wind and aligned roughly along contours of temperature or dynamic height. PDFs of meridional or cross-stream velocities (solid line) are centered near zero but are, on average, positive (see upper part of Table 1), implying northward transport at the surface. This is consistent with a mean Ekman transport oriented to the left of the Southern Ocean winds. The widths of the PDFs in Fig. 3 indicate that there is substantial variability about the mean. In particular, cross-stream surface motions may be difficult to distinguish from a random walk centered around the mean geostrophic streamlines.

Table 1 summarizes the statistics of the float velocities. The first part of the table shows mean velocities at the surface relative to geographic, dynamic height, and temperature contours. The second part indicates mean velocities at 900-m depth, estimated by projecting the float observations from depths between 700 and 1100 m onto the 900-m-depth surface, as discussed by Gille (2003). Along-stream surface float velocities are roughly 3 to 4 times greater than along-stream subsurface velocities. Thus, in 24 h at the surface, a float is likely to travel the same along-stream distance that it would in 3 or 4 days at 900-m depth. Cross-stream surface velocities are an order of magnitude larger than cross-stream subsurface velocities, which are barely distinguishable from zero at the 95% significance level. Thus, for a float that spends 10 days at 900 m for every 1 day at the ocean surface, at least 50% of cross-stream motions will be due to surface processes.

As a result of cross-stream surface motions, on average the surface temperature and dynamic height of the water surrounding the float will increase during the time that the float spends at the surface. In addition, when the float resubmerges, it is expected to return to a water mass that is warmer and has higher dynamic height than the water from which it came. To quantify these changes,

TABLE 1. Mean velocity of ALACE floats at the surface and at 900-m depth, relative to lines of latitude, dynamic height relative to 3000 m and temperature contours, where N is the number of observations, and reported errors of the mean are 2 times the std dev divided by $\sqrt{N}$. As discussed in the text, temperature and dynamic height at the surface and at 900-m depth are derived from hydrographic atlas data mapped by Gouretski and Jancke (1998).

Displacement	Zonal direction	Dynamic height contour	Temperature contour
	Surface velocity (cm s^{-1})		
N	15 027	12 329	14 813
Tangent (i.e., along-stream)	11.8 ± 0.4	11.5 ± 0.4	9.7 ± 0.4
Normal (i.e., cross-stream)	1.8 ± 0.3	1.9 ± 0.4	1.4 ± 0.4
	Velocity at 900-m depth (cm s^{-1})		
N	12 858	9255	11 747
Tangent (i.e., along-stream)	2.9 ± 0.2	3.2 ± 0.2	3.3 ± 0.2
Normal (i.e., cross-stream)	0.13 ± 0.12	−0.11 ± 0.14	−0.17 ± 0.12

TABLE 2. Mean changes in properties of ALACE floats in 24 h relative to temperature contours and geostrophic streamlines at the surface and 900-m depth relative to 3000 m, where N is the number of observations, and reported errors of the mean are 2 times the std dev divided by $\sqrt{N}$. As discussed in the text, temperature and dynamic height at the surface and at 900-m depth are derived from hydrographic atlas data objectively mapped by Gouretski and Jancke (1998).

	Dynamic height	Temperature
Change in properties at the surface during 1 day at the surface		
Mean	0.11 ± 0.03 cm	(1.1 ± 0.3) × 10^{-2}°C
N	12 176	14 694
Change in properties at 900 m resulting from 1 day at the surface		
Mean	(3.9 ± 1.3) × 10^{-2} cm	(3.1 ± 1.1) × 10^{-3}°C
N	12 176	14 355
Change in properties at 900 m during 1 day at 900 m		
Mean	(2.6 ± 4.8) × 10^{-3} cm	(2.5 ± 3.6) × 10^{-4}°C
N	9256	11 753

we interpolated time-averaged mean atlas data from Gouretski and Jancke (1998) onto the beginning and end points for the surface displacements.

Table 2 summarizes the average changes in dynamic height and temperature that would be expected as a result of 24-h displacements. The first part of the table shows the expected increase in surface properties. In a typical 24-h period at the surface, an ALACE float is expected to move into water that is 0.1 ± 1.6 dynamic centimeters higher and 0.01° ± 0.20°C warmer than the water where it started. (Error bars in Table 2 are errors of the mean, while results discussed here in the text are errors for single realizations.) The second part of the table shows that as a result of this surface advection, a float ballasted to 900-m depth would typically return to water that was 0.04 ± 0.71 dynamic centimeters higher and (3 ± 67) × 10^{-3}°C warmer than the water in which it floated in the previous cycle. The final segment of Table 2 shows the expected change in subsurface properties as a result of a 1-day displacement at 900-m depth. In contrast with surface velocities, subsurface velocities are on average oriented along mean dynamic height or temperature contours. In a statistically averaged sense, subsurface motions change neither the dynamic height nor the temperature of the water surrounding the floats.

In 2 years' worth of 10-day cycles, a float will spend about 70 days at the surface. These results indicate that in this time a typical float is likely to be displaced 540 ± 380 km eastward and 100 ± 270 km northward relative to a float that never rose to the surface. At 900-m depth, this is equivalent to an average change of 0.027 ± 0.120 dynamic meters and 0.22° ± 1.10°C. Thus for an individual float, the impact of spending time at the surface may not have a discernible pattern, but for the collective dataset, surface processes are likely to result in a northward advection and statistically significant change in temperature and dynamic height that could not be attributed to subsurface processes. Moreover, temperature and dynamic height shifts are likely to be largest where gradients are sharp, within the Antarctic Circumpolar Current. Surface displacements should be taken into account in computations of extended time period float behavior, and they are likely to be particularly important for conventional dispersion calculations that examine the statistics governing the gradual separation of two floats launched from the same location (e.g., Taylor 1921; LaCasce and Bower 2000).

4. Surface circulation from floats

Surface displacements may make long-term ALACE trajectories difficult to interpret, but they also have the potential to tell us about surface ocean circulation. Pazan and Niiler (2001, hereafter PN01) explored the possibilities of estimating the wind slip of undrogued surface drifters by comparing the wind responses of drogued and undrogued drifters. ALACE floats have roughly the same shape as drifters that have lost their drogues and are expected to behave in much the same way. Therefore, we have applied a method analogous to that of PN01 to investigate ALACE drift velocities at the ocean surface.

PN01 used two-dimensional complex regressions to determine the dependence of drogued and undrogued drifter velocities on wind speed. We use the same type of regression model to determine the dependence of ALACE float and drogued drifter velocities on winds. We seek relationships of the form

$$U_f = A_f + B_f W_f, \quad (1)$$

$$U_d = A_d + B_d W_d, \quad (2)$$

where U_f and U_d represent vector velocities of floats and drogued drifters, respectively, and W_f and W_d correspond to vector wind velocities that have been interpolated onto the float and drogued drifter positions and times. The regression coefficients A_f, A_d, B_f, and B_d are complex and can be represented using amplitudes and phase angles. For example, $A_f = |A_f| \exp(i\phi_{A_f})$.

a. Southern Ocean–wide average differences between drogued and undrogued motions

All available float and drogued drifter data were used to derive geographically averaged coefficients, provided that they fell within three standard deviations of the mean velocities and came from the region south of 30°S. Drifter data represent repeated measurements from the same instruments and are estimated to decorrelate on timescales of 2–4 days. Therefore, we assumed that one-third of drifter observations were statistically independent. In contrast, since surface float observations are separated in time by at least 8 days, all float observations were assumed to be statistically independent. Table 3 summarizes the magnitudes and angular orientations of the fitted coefficients. The angle of B, ϕ_B, is larger for the drogued drifter data than it is for the ALACE floats,

TABLE 3. Magnitude and angle of regression coefficients from Eqs. (1) and (2), where N is the number of observations. Mean wind velocities at float and drifter locations are also indicated. Observations used in this analysis are drawn from the latitude range between 30° and 60°S.

	ALACE floats	Drogued drifters
$\|A\|$	$(54.0 \pm 1.0) \times 10^{-3}$ m s^{-1}	$(30.0 \pm 0.1) \times 10^{-3}$ m s^{-1}
ϕ_A	18.0° ± 0.7°	10.1° ± 0.1°
$\|B\|$	$(130.0 \pm 1.0) \times 10^{-4}$	$(67.0 \pm 0.1) \times 10^{-4}$
ϕ_B	16.3° ± 0.3°	33.9° ± 0.1°
N	14 346	244 269
Zonal wind	4.67 ± 0.09 m s^{-1}	3.28 ± 0.04 m s^{-1}
Meridional wind	−1.15 ± 0.08 m s^{-1}	−0.63 ± 0.04 m s^{-1}

implying that drogued drifters are advected more clearly to the left of the wind than are floats. This is not surprising, since the drogues of the drifters are deeper within the Ekman layer than the surface floats are, so drogued drifters should roughly follow the motions of water 15 m below the surface.

b. *Undrogued versus drogued motions in geographic subregions*

In situations where $W_f = W_d$ the difference between (2) and (1) represents the difference between float and drifter motions:

$$U_f - U_d = A_f - A_d + (B_f - B_d)W_f = A_\Delta + B_\Delta W_f \quad (3)$$

(see PN01). In this case, the expected motions of a drogued drifter can be predicted using the measured surface float motions U_f and wind velocity W_f along with the coefficients A_Δ and B_Δ. As Table 3 indicates, the mean winds for the full Southern Ocean, W_f and W_d, are not the same within standard errors and differ by more than 50%. Therefore, we did not apply (3) to the statistics reported in Table 3 but instead carried out our analysis in geographic regions in which W_f and W_d were similar in value.

Following the framework developed by PN01, we sorted the float and drifter data collected between 30° and 60°S into 2° latitude by 8° longitude (2 × 8) bins. Since Southern Ocean flow is predominantly zonal, we also considered 1° latitude by 360° longitude (1 × 360) bins. For each bin we computed separate sets of regression coefficients. PN01 selected 2 × 8 bins for further analysis only if they met specified statistical criteria, and we applied these criteria where possible. Bins were selected for further analysis if they contained at least 25 float observations and if no more than 20% of the drifter observations were provided by a single drifter. In addition, the difference between the wind speeds for drifters and floats was required to be 1 m s^{-1} or less, and the float and drifter mean wind directions could differ by no more than 30°. PN01 also mandated that the mean winds be between 3 and 8 m s^{-1}, but this criterion proved impractical in the Southern Ocean since it would have eliminated all of the bins located in the ACC region. As with the mean coefficients derived above, float and drifter velocities were excluded from the calculation if they differed from the local mean by more than three standard deviations.

Figure 4 shows estimates of the magnitudes ($|A_\Delta|$ and $|B_\Delta|$) and angular orientations (ϕ_{A_Δ} and ϕ_{B_Δ}) of the regression coefficients as a function of latitude for the 2 × 8 bins and for the 1 × 360 bins. For the 2 × 8 case, the regression model explains about 13% of the rms float variability and 3% of the rms drifter variability, while for the 1 × 360 case it captures 12% of the rms float variability and 4% of the rms drifter variability. The large fraction of variability that is not explained by the regressions is attributed to a variety of processes, including eddy variability and observational error.

The amplitude $|A_\Delta|$ estimates the constant difference between float and drifter speeds at the same location and experiencing the same wind conditions. In their earlier comparisons of drogued and undrogued drifters, PN01 reported that $|A_{\Delta_{PN}}| = 0$ m s^{-1}. In contrast, in these float–drifter comparisons, $|A_\Delta|$ was statistically different from zero at the 95% level in most bins. Figure 4a shows estimates of $|A_\Delta|$ as a function of latitude. The amplitude of the weighted mean average, $|\overline{A}_\Delta|$, is 0.012 ± 0.002 m s^{-1} for 2 × 8 bins and 0.016 ± 0.001 m s^{-1} for 1 × 360 bins. Here and throughout the remainder of this section, means are computed using formal error bars from the regression to weight estimates from each bin. This is roughly equivalent to weighting each bin by the number of available observations. Nonzero values of $|\overline{A}_\Delta|$ may indicate that drifters and ALACE floats respond differently to surface currents, which are not part of the regression model, or the offset may stem from deficiencies in the available wind observations. No strong latitudinal dependence is shown by $|A_\Delta|$, suggesting no simple geographic origin for the mean offset.

The angular orientation estimate ϕ_{A_Δ} indicates the orientation difference between constant (nonwind forced) components of the float and drogued drifter velocities. Individual angular differences, shown in Fig. 4b, span a broad range of values. The weighted mean of the phase, $\phi_{\overline{A}_\Delta}$, is 71° ± 6° for 2 × 8 bins and 46° ± 6° for 1 × 360 bins. The fact that these differ from zero indicates that the background drifts of the floats and drifters are not necessarily oriented in the same direction, possibly because of spatial or temporal sampling differences for the two datasets.

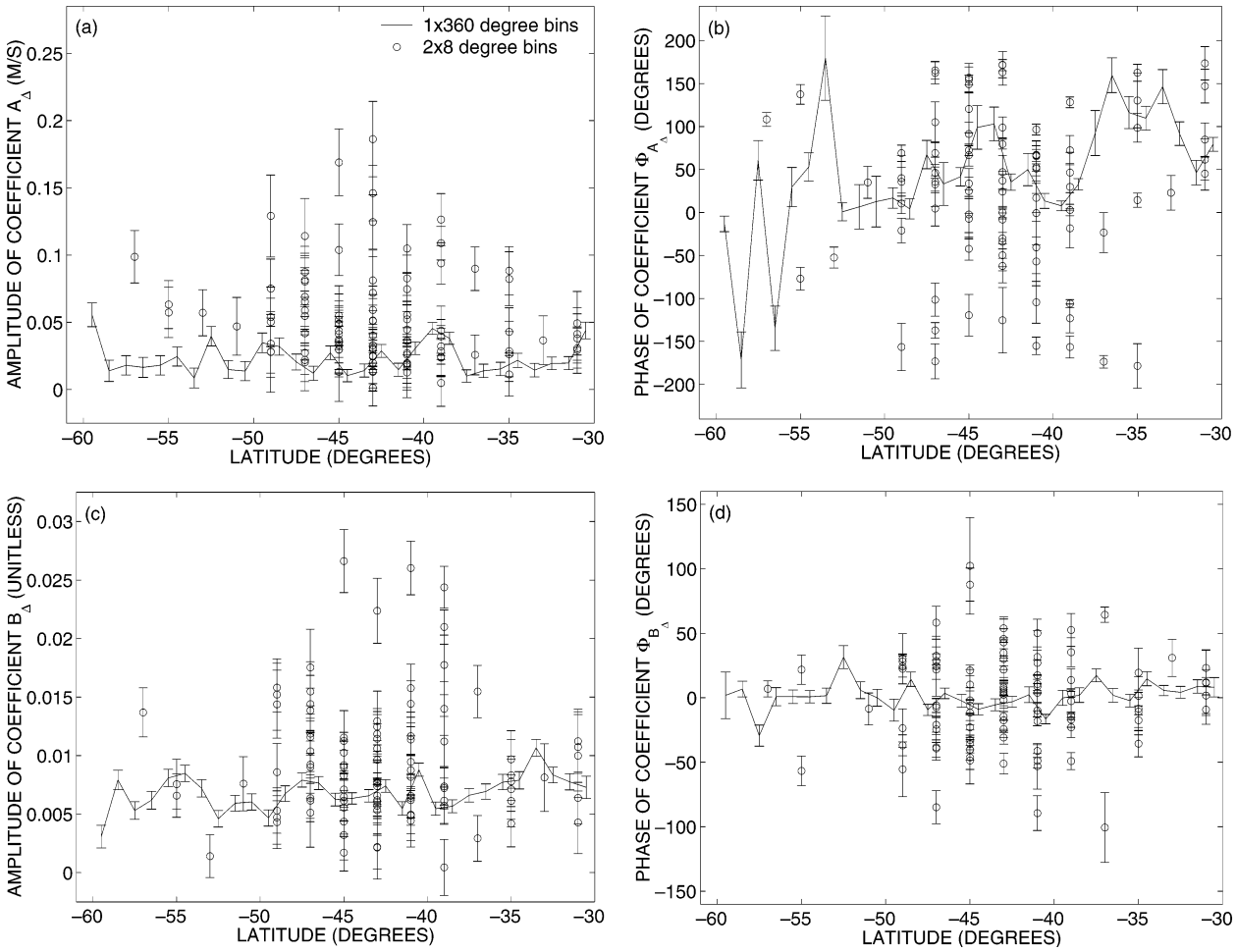

FIG. 4. Magnitude and angle of the difference between regression coefficients computed for ALACE float and drogued drifter velocities as functions of wind speed. Regression coefficients were computed in bins with dimensions 2° lat by 8° lon (open circles) and 1° lat by 360° lon (solid line). Their magnitudes and phases are shown as functions of latitude. Error bars indicate 95% confidence intervals. (a) Magnitude of the constant offset, $|A_\Delta|$. (b) Orientation angle of the constant offset, ϕ_{A_Δ}. (c) Amplitude of the wind coefficient, $|B_\Delta|$. (d) Angular orientation of the wind coefficient, ϕ_{B_Δ}.

ALACE floats are strongly influenced by winds. In Fig. 4c, $|B_\Delta|$ quantifies the expected deviation between drifters and floats due to wind forcing. The amplitude of the weighted mean of PN01's $B_{\Delta_{PN}}$ is $(7.9 \pm 0.1) \times 10^{-3}$. In our analysis, for 2×8 bins, the weighted mean of B_Δ has a magnitude of $(7.7 \pm 0.2) \times 10^{-3}$, which agrees with the mean of PN01's within error bars. For 1×360 bins the absolute value of the weighted mean $\overline{B}_\Delta$ is $(6.7 \pm 0.1) \times 10^{-3}$, slightly lower than the mean obtained from the analysis of 2×8 bins. Neither the 2×8 bins nor the 1×360 bins show a trend with latitude.

For both 2×8 and 1×360 bins, in Fig. 4d, the angles ϕ_{B_Δ} are near zero with no latitudinal dependence. The phase of the weighted means, $\phi_{\overline{B}_\Delta}$, is $-3.5° \pm 1.0°$ for 2×8 bins and $0.6° \pm 1.0°$ for 1×360 bins, while PN01's estimate of $-1.4° \pm 0.4°$ lies in between these two estimates. This suggests that wind-forced undrogued motion is aligned in the direction of the wind.

Since none of the coefficients depend strongly on latitude, and the 2×8 bin results are based on fewer observations and are therefore broadly scattered, the best estimates of A_Δ and B_Δ are the weighted mean values from the 1×360 case:

$$|\overline{A}_\Delta| = 0.016 \pm 0.001 \text{ m s}^{-1}, \qquad \phi_{\overline{A}_\Delta} = 46° \pm 3°,$$
$$|\overline{B}_\Delta| = (0.67 \pm 0.01) \times 10^{-2}, \qquad \phi_{\overline{B}_\Delta} = 0.6° \pm 1.0°. \tag{4}$$

Although formal error bars for the coefficients are small, statistical errors are likely to be large for each individual realization, because of the large variances in the wind and float velocity fields and also because of uncertainties in wind fields and background flow. Therefore, estimates of drogued drifter behavior made from undrogued ALACE floats are likely to be noisy. Uncertainties in mean flow fields should drop like $1/\sqrt{N}$, so that large-scale flow patterns derived from many independent obser-

vations may depict the mean large-scale flow realistically. These mean fields are likely to be particularly valuable in regions of the world where surface flows are otherwise difficult to sample.

5. Summary

This study has analyzed the behavior of ALACE floats at the surface of the Southern Ocean. All of the floats deployed during the 1990s as part of the World Ocean Circulation Experiment relied on Argos system satellites to transmit their data to land. Transmission required that the floats spend 24 h at the surface during each float cycle of 10–25 days.

Because of windage and the Ekman effect, during their time at the surface Southern Ocean floats tended to move northward relative to temperature isolines, dynamic height contours, and lines of latitude. Nonetheless, even in the high-wind region of the Southern Ocean, floats tend to travel farther along streamlines than across them. This analysis indicates that in the course of 70 days at the surface, representing 2 years' worth of 10-day cycles, a typical float would move 540 $\pm$ 380 km eastward and 100 $\pm$ 270 km northward relative to a float that never surfaced. As a result of this northward displacement, the mean temperature of a 900-m-deep float would be expected to increase by 0.22° $\pm$ 1.10°C and the mean dynamic height to rise by 0.027 $\pm$ 0.120 dynamic meters.

Surface float motions are statistically correlated with NCEP winds at the 95% level. In least squares fits to wind velocity data, floats, which are undrogued, have larger regression coefficients than drogued drifters, indicating that the floats respond more strongly to wind than drifters do. Differences between float and drifter regression coefficients are constant as a function of latitude. Using derived coefficients, the upper-ocean currents seen by drogued drifters can be reconstructed from undrogued floats in combination with wind fields.

The successors to ALACE, dubbed Argo floats, will be deployed extensively over the next decade to monitor global climate variability. Argo planners hope to take advantage of new global telecommunications satellites in order to shorten the time period that the floats need to spend at the ocean surface, which would make long-term dispersion analysis possible using float data. Logistical and financial difficulties faced by the global satellite programs may delay the implementation of high-speed telecommunications systems and yield an extended dataset of day-long surface displacements. Results of this study suggest that these surface velocity records can be used as a noisy complement to surface drifter datasets. Ultimately, if global satellite coverage is available, Argo floats are likely to spend an hour or less at the surface during each cycle. If sufficient data were available, even short-duration surface displacements could be used to detect surface currents, although the inferred velocities would be sensitive to small positioning errors and therefore might be difficult to interpret.

Acknowledgments. We are grateful to Russ Davis for making Southern Ocean ALACE floats available and to Peter Niiler and Sharon Lukas for providing surface drifter data. NCEP reanalysis data was provided by the NOAA–CIRES Climate Diagnostics Center, Boulder, Colorado, from their Web site at http://www.cdc.noaa.gov/. This research was funded by NSF Award OCE-9985203/OCE-0049066.

REFERENCES

Davis, R. E., 1992: The Autonomous Lagrangian Circulation Explorer (ALACE). *J. Atmos. Oceanic Technol.,* **9,** 264–285.

——, 1998: Preliminary results from directly measuring middepth circulation in the tropical and South Pacific. *J. Geophys. Res.,* **103,** 24 619–24 639.

——, P. D. Killworth, and J. R. Blundell, 1996: Comparison of Autonomous Lagrangian Circulation Explorer and fine resolution Antarctic model results in the South Atlantic. *J. Geophys. Res.,* **101,** 855–884.

Gill, A. E., 1982: *Atmosphere–Ocean Dynamics.* Academic Press, 662 pp.

Gille, S. T., 2003: Float observations of the Southern Ocean. Part I: Estimating mean fields, bottom velocities, and topographic steering. *J. Phys. Oceanogr.,* **33,** 1167–1181.

Gouretski, V. V., and K. Jancke, 1998: A new climatology for the World Ocean. WOCE Special Analysis Centre, Max-Planck Institut, WHP SAC Tech. Rep. No. 3, WOCE Report No. 162/98, Hamburg, Germany.

Kalnay, E., and Coauthors, 1996: The NCEP/NCAR 40-Year Reanalysis Project. *Bull. Amer. Meteor. Soc.,* **77,** 437–471.

LaCasce, J. H., 2000: Floats and f/H. *J. Mar. Res.,* **58,** 61–95.

——, and A. Bower, 2000: Relative dispersion in the subsurface North Atlantic. *J. Mar. Res.,* **58,** 863–894.

McNally, G. J., and W. B. White, 1985: Wind driven flow in the mixed layer observed by drifting buoys during autumn-winter in the midlatitude North Pacific. *J. Phys. Oceanogr.,* **15,** 684–694.

Niiler, P. P., A. S. Sybrandy, K. Bi, P. M. Poulain, and D. Bitterman, 1995: Measurements of the water-following characteristics of Tristar and Holey-sock drifters. *Deep-Sea Res.,* **42,** 1951–1964.

O'Dwyer, J. O., R. G. Williams, J. H. LaCasce, and K. G. Speer, 2000: Does the potential vorticity distribution constrain and spreading of floats in the North Atlantic? *J. Phys. Oceanogr.,* **30,** 461–474.

Pazan, S. E., 1996: Intercomparison of drogued and undrogued drift buoys. *Proc. Oceans '96,* Vol. 2, Fort Lauderdale, FL, MTS/IEEE, 864–872.

——, and P. P. Niiler, 2001: Recovery of near-surface velocity from undrogued drifters. *J. Atmos. Oceanic Technol.,* **18,** 476–489.

Taylor, G. I., 1921: Diffusion by continuous movements. *Proc. London Math. Soc.,* **20,** 196–212.